Thermochimica Acta, 195 (1992) 261–275
Elsevier Science Publishers B.V., Amsterdam

The application of DSC to the study of phase segregation during the thermal cycling of *para*-dihalosubstituted derivatives of benzene and their alloys

M. Labrador [a], M.A. Cuevas-Diarte [a], D. Mondieig [b] and Y. Haget [b]

[a] *Dep. Cristallografia, Mineralogia i Dipòsits Minerals, Fac. Geologia Universitat de Barcelona, c/Martí i Franqués, s/n, E-08028 Barcelona (Spain)*
[b] *Lab. Cristallographie et Physique Cristalline, URA 144 CNRS Université Bordeaux I, 351, Cours de la Libération, F-33405 Talence (France)*

(Received 17 May 1991)

Abstract

Calorimetric techniques are most commonly used in our research into organic compounds and their alloys, both for the initial characterization of the products and for the determination of phase diagrams that may be established. They are equally useful for the cycling of materials used for energy storage by latent heat, and for the study of their behaviour. This paper also demonstrates the use of the DSC technique to study the homogeneity of these materials when they are subjected to continuous thermic cycling.

INTRODUCTION

This paper forms part of a study into energy storage by latent heat using organic materials [1], in both pure and alloyed forms, which are called MAPCM (Molecular Alloy Phase Change Materials).

In previous papers we have reported the results from the different types of studies carried out: cycling on a milligram scale [2] carried out by DSC [2], and cycling on a gram scale [3]. We have also analysed segregation of the compositional phases that the material may undergo during the process, as well as the overall behaviour of the materials.

A particular aspect of the study of segregation is presented in which we show how DSC clearly demonstrates the evolution of the compositional homogeneity of the samples studied. With this technique we can characterize the initial constituents in terms of temperature and phase-change energy, and so obtain results directly in the case of small-scale thermic cycling of the samples [4–6]. Using DSC, we can obtain precise knowledge of the resulting phase diagrams: the different equilibrium regions, phase transitions and associated temperatures. Furthermore we can also obtain the shape of the thermic signal for the different compositions. Analysis of

the evolution of the shape of the melting peaks during a thermic cycle and for differents zones of the overall cycled sample, provides qualitative information regarding the evolution of compositional homogeneity. The DSC signal varies its position (in temperature), indicating a variation in the characteristic temperature, and/or varies its shape, becoming wider or narrower according to the width of the solid–liquid interval (or intervals if segregation has occurred). It may even be possible to quantify the homogeneity of the sample studied [3] if the phase diagram is known beforehand.

EXPERIMENTAL METHODOLOGY

The conditions described by Chevalier et al. [7] were taken as a starting point. Two types of cycle were employed: a long one of 4 h (2000 cycles) and a shorter one of 1/2 h (10 000 cycles).

The material was arranged inside hermetically sealed Pyrex tubes 12.5 mm wide and 70 mm long (12–15 g of product depending on the composition). The tubes were arranged both vertically and horizontally for cycling (for further information see ref. 3). Hereafter, we shall refer to long-vertical cycles, long-horizontal cycles, short-vertical cycles or short-horizontal cycles.

To study the compositional homogeneity of the alloys during cycling, sampling of the tubes was carried out in both longitudinal and transversal directions. Figure 1 shows the distribution and nomenclature of the different zones. From each of these we took three independent samples after

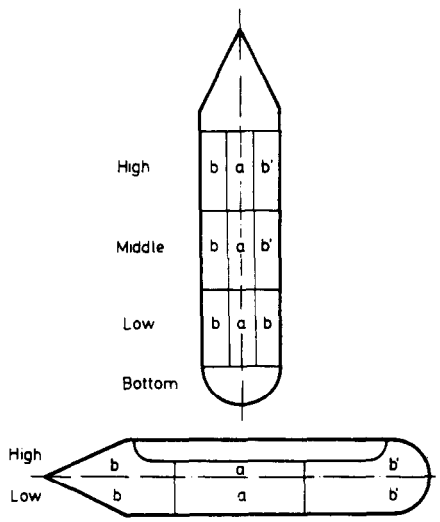

Fig. 1. Distribution and nomenclature of the different analysed zones.

each n cycles and proceeded to analyse them by DSC using a Perkin–Elmer DSC-4.

MATERIALS STUDIED

The initial constituent materials of the alloys studied are benzene para-disubstitutes: *para*-dichlorobenzene (pDCB), *para*-dibromobenzene (pDBB) and *para*-bromochlorobenzene (pBCB). Figure 2 shows a fusion signal pattern obtained by DSC for these compounds.

The following phase diagrams formed have been determined by our group: pDCB–pDBB [8,9], pDCB–pBCB [10,11] and pBCB–pDBB [12,13]. This paper gives results for compositions of the first two systems, for which we discuss certain aspects of interest.

p*DCB*–p*BCB system*

There is complete miscibility is total between room temperature and fusion (Fig. 3). A small eutectic invariant is shown due to the polymorphism of pDCB. The solid–liquid range and consequent energy storage interval for the different alloys is remarkably narrow, never rising above 1°C. Thus

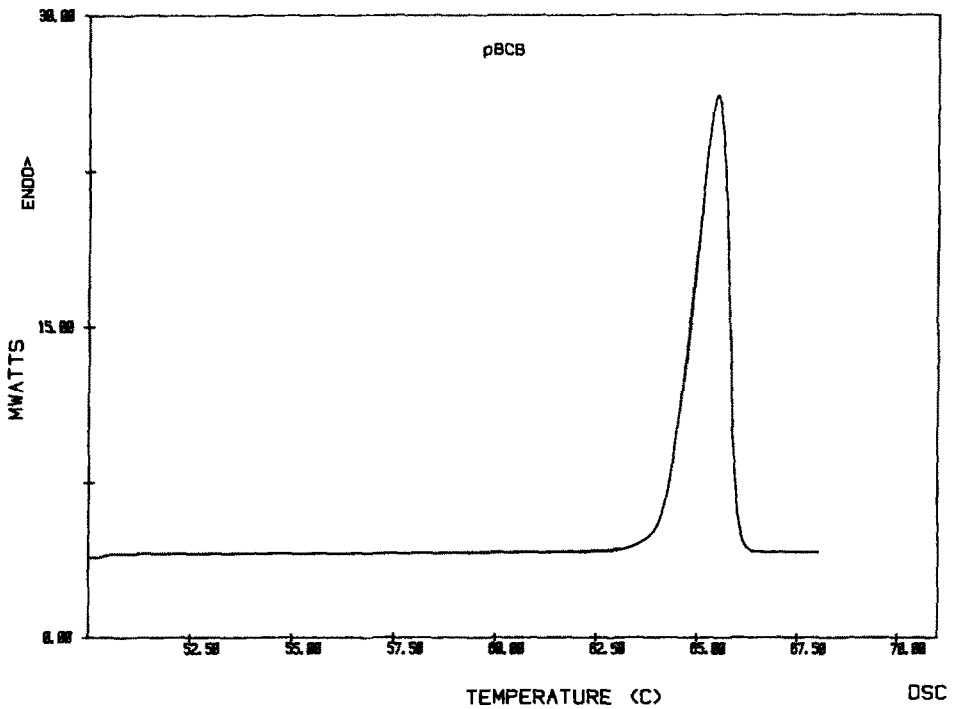

Fig. 2. DSC fusion signal for pBCB.

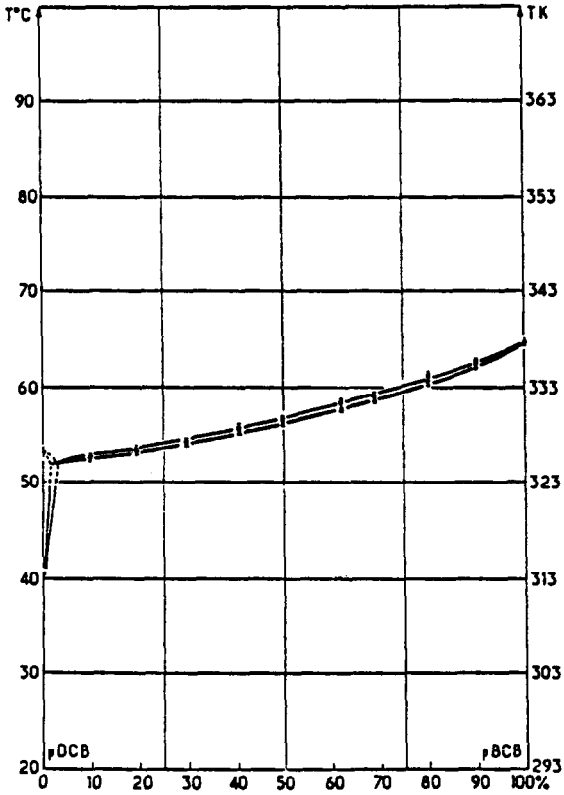

Fig. 3. pDCB–pBCB phase diagram.

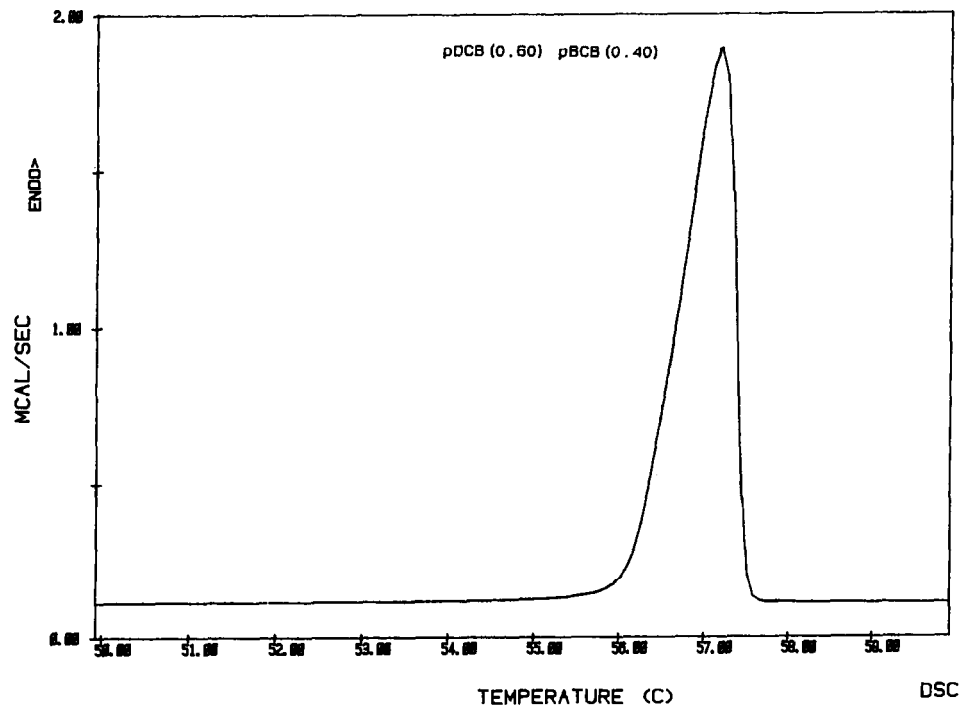

Fig. 4. DSC fusion signal for $p\mathrm{DCB}_{0.60}p\mathrm{BCB}_{0.40}$ alloy.

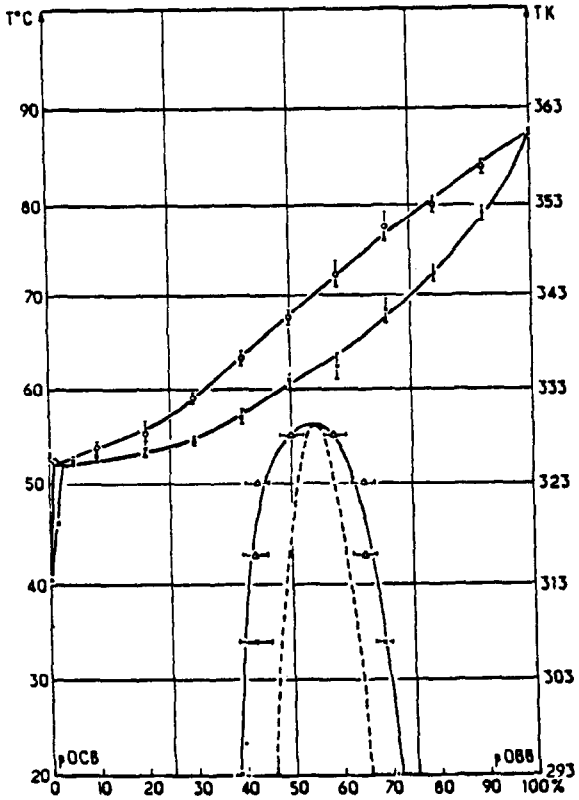

Fig. 5. pDCB–pDBB phase diagram.

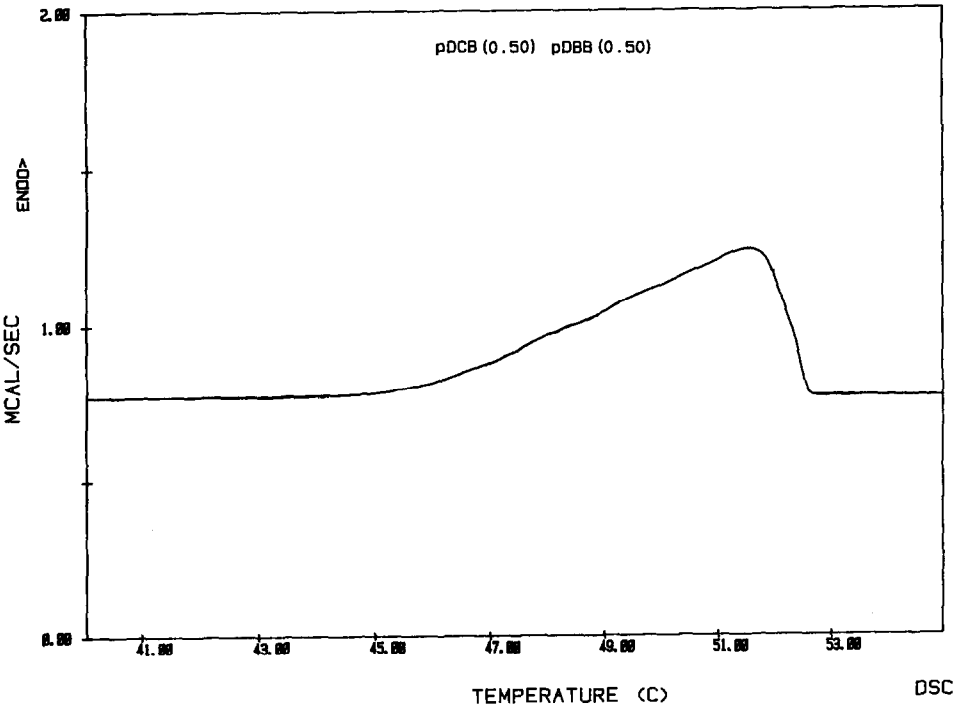

Fig. 6. DSC fusion signal for $p\mathrm{DCB}_{0.50}p\mathrm{DBB}_{0.50}$ alloy.

the DSC signals of the alloys (Fig. 4) are very similar in shape and surface to those of the initial compounds, with similar energy levels (183 MJ m^{-3}).

p*DCB*–p*DBB system*

The phase diagram (Fig. 5) shows a relatively wide immiscibility gap at room temperature (33%), but solubility is total at high temperature. Here the eutectic invariant is also very restricted to compositions close to *p*DCB. Fusion of the alloys takes place over a fairly narrow interval for concentrations close to those of the initial constituents but this interval widens for the central concentrations and may reach 9°C, giving rise to fusion signals of rather different shape from those of the initial products, as can be seen in Fig. 6 for the equimolar alloy of this system. The fusion enthalpy varies gradually between extremes of 183–196 MJ m^{-3}.

RESULTS

A more representative selection of the widths of the different fusion intervals for all the products analysed is: *p*BCB, isothermic fusion; $p\text{DCB}_{0.60}p\text{BCB}_{0.40}$ alloy, representing compositions with a narrow fusion interval, 1°C; $p\text{DCB}_{0.80}p\text{DBB}_{0.20}$ alloy, representing compositions with intermediate fusion intervals, 2°C, and $p\text{DCB}_{0.50}p\text{DBB}_{0.50}$ alloy, which shows a wide fusion interval (7–8°C) and which also belongs to the immiscibility zone of its phase diagram.

The DSC peaks shown are the averages of three independently measured samples in each case.

p*BCB*

Fig. 7 shows the DSC signals corresponding to the long-vertical cycle analysis; it can be seen that peaks of successively analysed cycles maintain their initial characteristics, which are identical for all the zones analysed, with narrow peaks situated in the same temperature band. The product therefore retains its initial thermic characteristics in a homogeneous manner over the 2000 cycles carried out.

p$DCB_{0.60}$p$BCB_{0.40}$

Figure 8 shows the results corresponding to the long-vertical cycle for this alloy. Apart from a slight displacement (not more than 1°C) towards higher temperatures in the central zones of the middle and upper parts of the tubes, the peaks do not evolve during cycling in either temperature displacement or shape. Therefore, this alloy undergoes no evolution during thermic cycling, behaving in practice like the initial product.

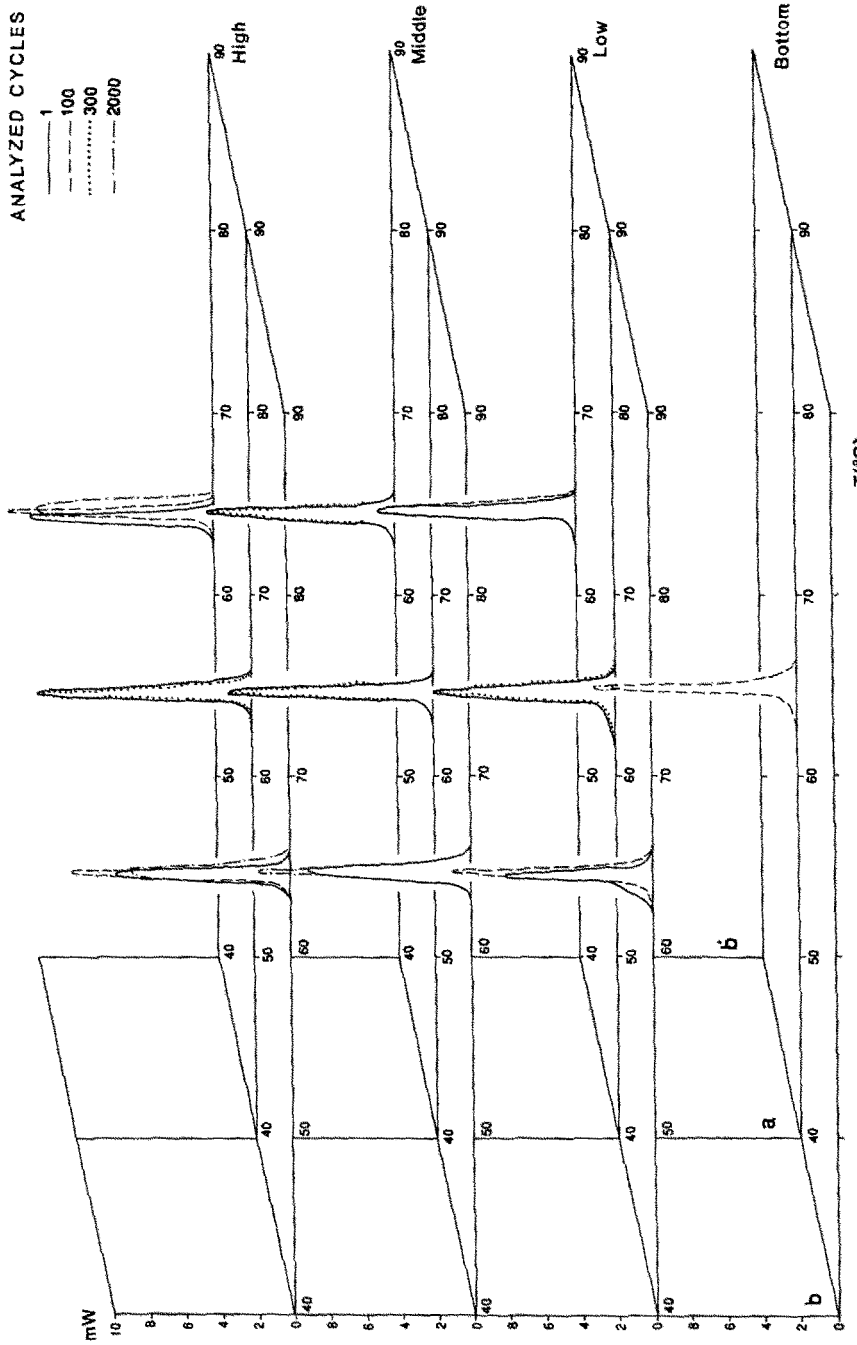

Fig. 7. DSC signals corresponding to the long-vertical cycle analysis for *p*BCB.

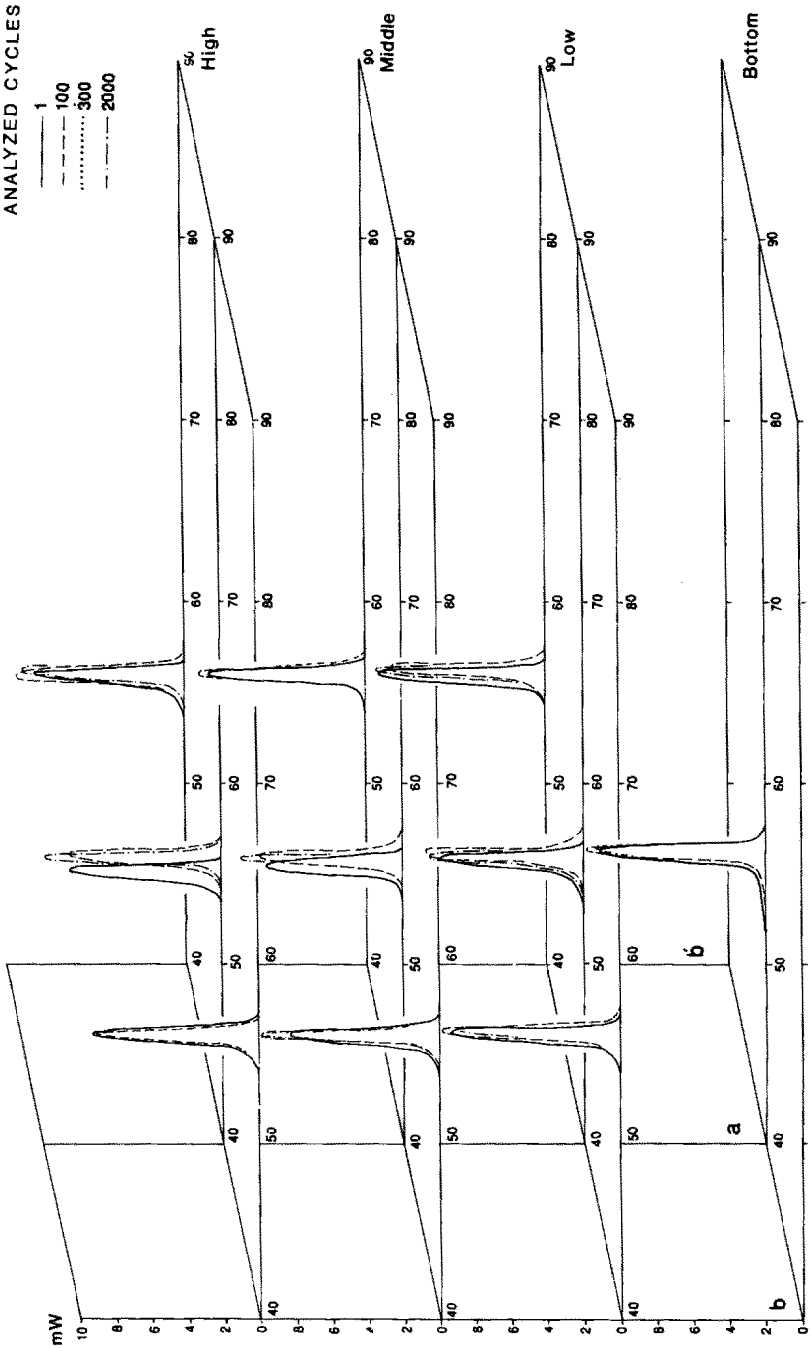

Fig. 8. DSC signals corresponding to the long-vertical cycle analysis for $pDCB_{0.60}pBCB_{0.40}$ alloy.

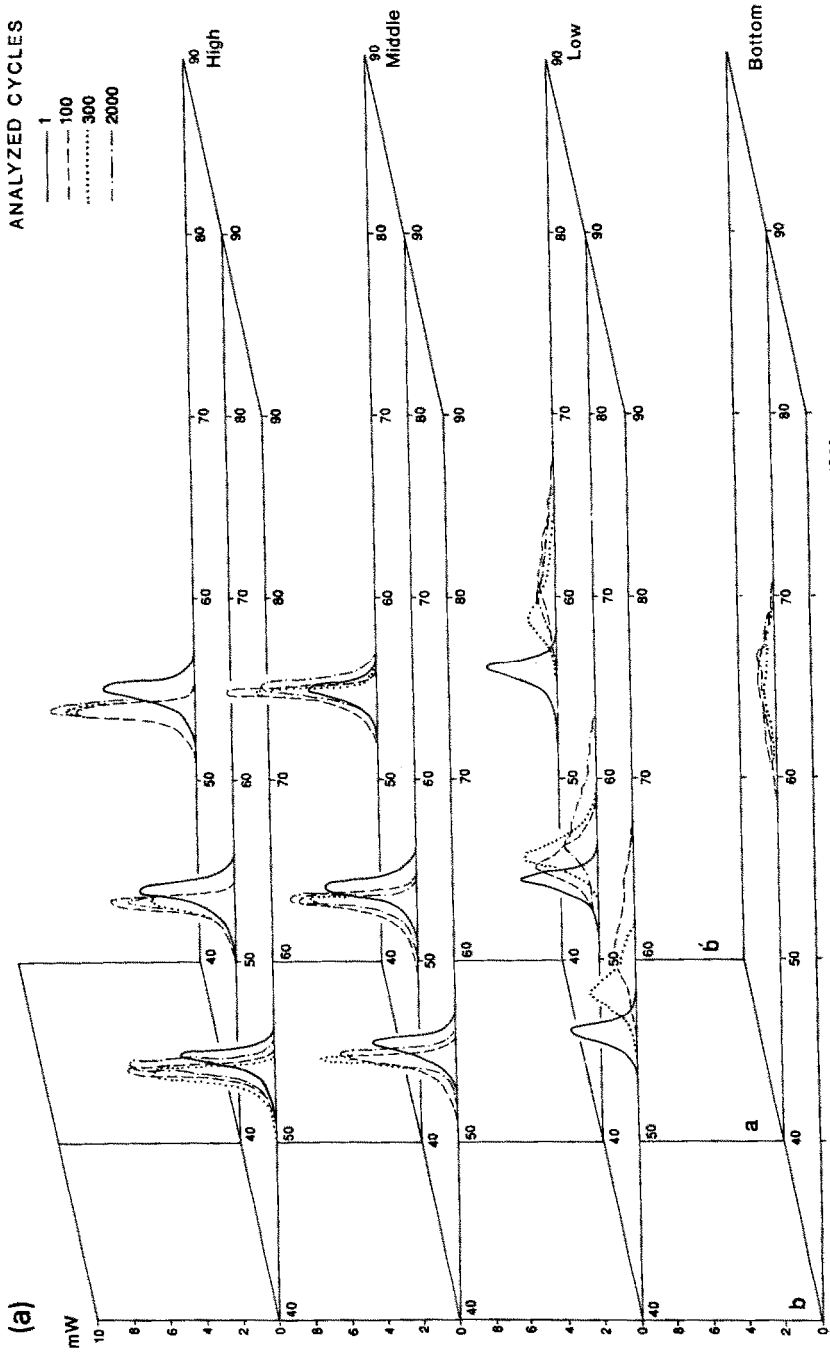

Fig. 9a. DSC signals corresponding to the long-vertical cycle analysis for $p\mathrm{DCB}_{0.80}p\mathrm{DBB}_{0.20}$ alloy.

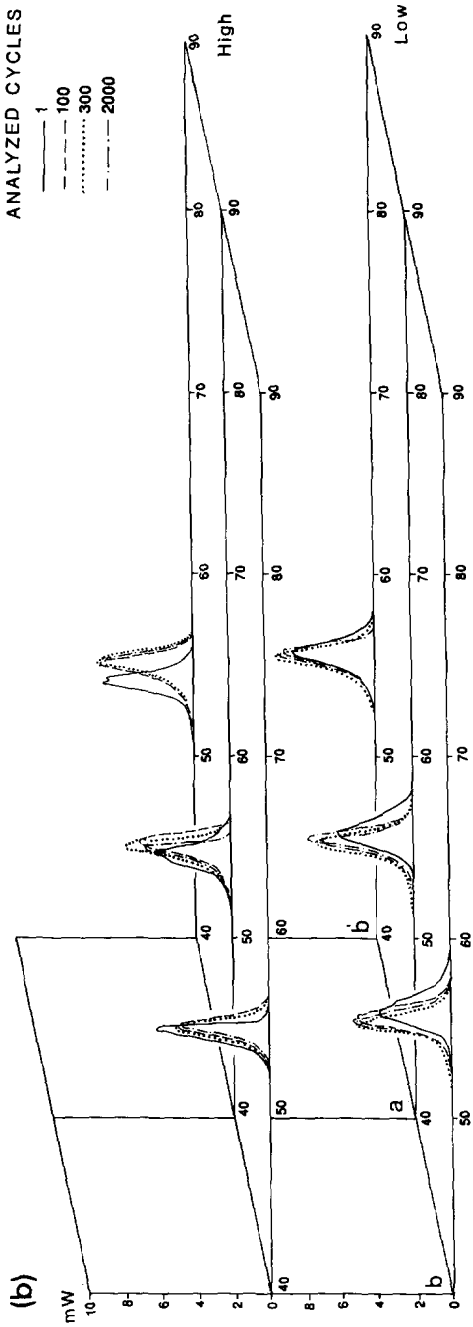

Fig. 9b. DSC signals corresponding to the long-horizontal cycle analysis for $p\mathrm{DCB}_{0.80}p\mathrm{DBB}_{0.20}$ alloy.

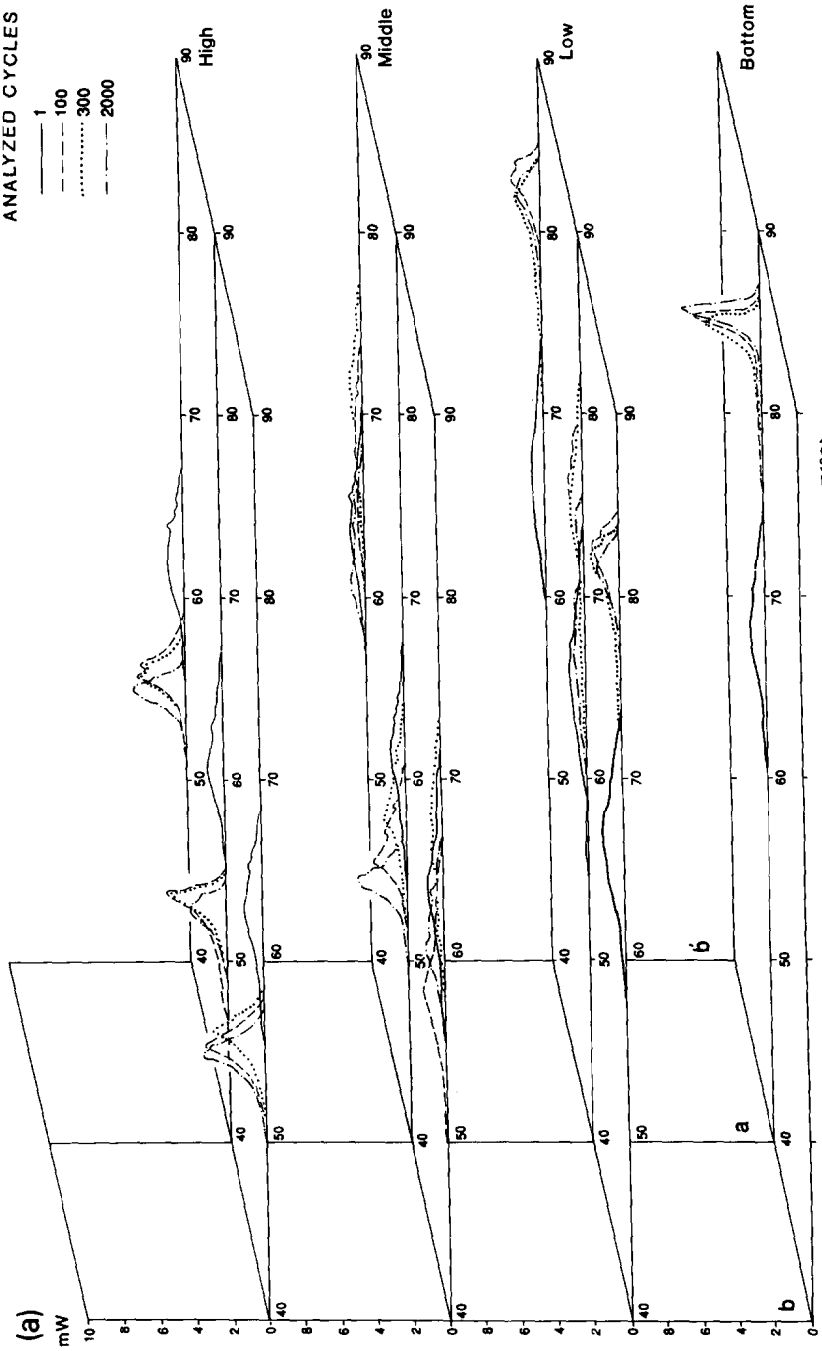

Fig. 10a. DSC signals corresponding to the long-vertical cycle analysis for $p\mathrm{DCB}_{0.50}$ $p\mathrm{DBB}_{0.50}$ alloy.

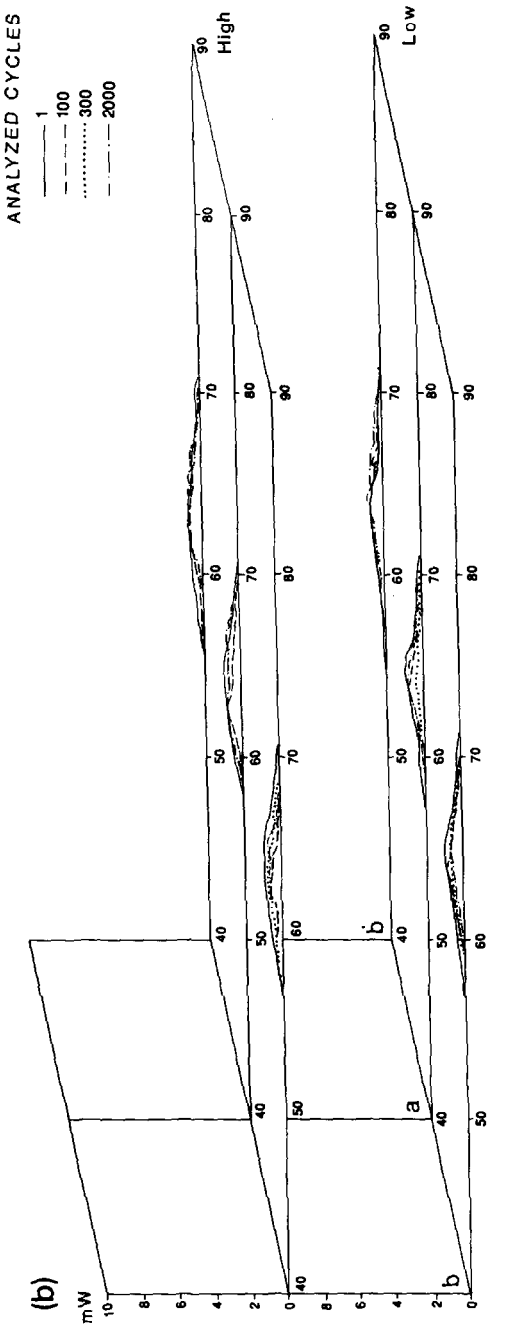

Fig. 10b. DSC signals corresponding to the long-horizontal cycle analysis for $p\mathrm{DCB}_{0.50}p\mathrm{DBB}_{0.50}$ alloy.

p$DCB_{0.80}$p$DBB_{0.20}$

The long-vertical (Fig. 9a) and long-horizontal (Fig. 9b) cycles are shown for this alloy. In contrast to the previous cases, the common characteristic is variation in both the temperature and in the shape of the thermic signals, a variation which differs with the arrangement of the cycling. The most important alteration is found in the long-vertical cycle, where different behaviour can be seen according to zone. Similarly, in the high and middle zones there is a slight displacement towards lower temperatures (1°C) at the same time as the respective peaks become narrower and higher; these differences tend to appear in the first cycles and remain stable in successive cycles. On the other hand, in the low zones and at the bottom, displacement is towards higher temperatures and is more pronounced (up to 4°C); the peaks become wider and lower, especially at the bottom. In the long-horizontal cycle, "movement" of the signals is weaker and the displacement follows no pattern as far as direction or shape is concerned, which may be indistinctly wider or sharper.

p$DCB_{0.50}$p$DBB_{0.50}$

Here results for the long-vertical (Fig. 10a) and long-horizontal (Fig. 10b) cycles are shown. The highest variation in temperature and signal shape of the four products studied is observed in the vertical cycle. Temperature displacement reaches 30°C for the samples taken from the bottom of the tube. The shape of the peaks is also very variable, with broad peaks in the first cycles that become successively sharper and more precise, especially those corresponding to the top and bottom of the tube, which is where the most extreme temperatures are found: 55 and 85°C respectively. This is almost the fusion temperature of the initial compounds: 53°C for *p*DCB and 87°C for *p*DBB, which indicates the magnitude of segregation that this alloy can reach. In the horizontal cycle, the behaviour is rather different: here no variation in temperature or signal shape is seen during cycling, which suggests that segregation is practically non-existent in this case.

DISCUSSION

Variations in fusion signals during cycling follow two distinct patterns: either they do not vary during the process, or else they show variation in temperature and shape that are related, on the one hand, to the width of the phase diagram and the temperature difference between the initial compounds and, on the other hand, to the disposition of the vessel during cycling (vertical or horizontal).

The first type of fusion signal reflects the isothermic equilibrium of the initial compounds (for instance, *p*BCB in Fig. 7) in which there is no evolution during cycling.

In the second type, corresponding to alloys, well differentiated situations are found: the case in which there is little variation, independent of the positioning of the containing vessel, because the alloy has a very narrow fusion loop ($p\mathrm{DCB}_{0.60}p\mathrm{BCB}_{0.40}$); and the case in which variation is very important ($p\mathrm{DCB}_{0.50}p\mathrm{DBB}_{0.50}$) and reflects the different solid–liquid equilibria that occur in crossing a wide fusion interval. Naturally, in the last situation the disposition of the containing vessel plays an important role, as the variation of the vertical dimension of the cycled material directly influences the extent of separation of the different solids formed during crystallization and therefore the rank of rehomogenization during the cycling. In this situation, the difference in densities between the initial products becomes important (1.52 g cm^{-3} for *p*DCB and 2.29 g cm^{-3} for *p*DBB), as, therefore, does the difference in densities between the different alloys that may appear during the cyclic fusion/crystallization process. One intermediate case appears in the $p\mathrm{DCB}_{0.80}p\mathrm{DBB}_{0.20}$ alloy for which the variation of the signals in the different parts of the tube is smaller because it corresponds to the narrowest fusion interval that the phase diagram shows for this composition.

CONCLUSIONS

The DSC technique is normally an indispensable tool in determining phase diagrams. In this paper, we have illustrated another potential use of this technique, which inverts that previously described. In this way, beginning with the knowledge of the phase diagrams and the close relation between fusion loops (in our case) and the different types of associated calorimetric signals, we can determine the different phases present in the fusion/crystallization processes studied. In short, this constitutes a good indirect method for obtaining the compositions of the samples analysed and, thereby, of discovering the homogeneity of an alloy with reasonable accuracy.

ACKNOWLEDGEMENTS

Financial support from the Fuerzas Eléctricas de Cataluña (FECSA), CAICYT (proyecto n° PR 84-0835) and Acción Integrada hispano-francesa is gratefully acknowledged.

REFERENCES

1 D. Mondieig, Y. Haget, M. Labrador, M.A. Cuevas-Diarte, P.R. van der Linde and H.A.J. Oonk, Mater. Res. Bull., in press.

2 M. Labrador, E. Tauler, M.A. Cuevas-Diarte, D. Mondieig, J.R. Housty and Y. Haget, Mater. Res. Bull., in press.
3 M. Labrador, T. Calvet and M.A. Cuevas-Diarte, D. Mondieig, J.R. Housty and Y. Haget, Mater. Res. Bull., 26 (1991) 749.
4 S. Cantor, Thermochim. Acta, 26 (1978) 39–47.
5 J.P. Elder, Thermochim. Acta, 36 (1980) 67–77.
6 G.A. Lane, J.S. Best, E.C. Clarke, D.N. Glew, G.C. Karris, S.W. Quigley and H.E. Rosow, Solar energy subsystems employing isothermal heat sink materials, Dow Chemical Co., Report NSF/RANN/SE/C906/FR/76/2, Midland, MI, 1976.
7 J.L. Chevalier, P. Eurin, J. Guion, H. Sallée, J.D. Sylvain and M.J. Wetterwald, Cah. Cent. Sci. Tech. Batim., University of Grenoble, 1983, Cah. 1892, livraison 244. 244 (1983) 1982.
8 A. Maiga, Thèse 3ème Cycle, University of Bordeaux I, 1983.
9 Y. Haget, J.R. Housty, A. Maiga, L. Bonpunt, N.B. Chanh, M.A. Cuevas-Diarte and E. Estop, J. Chim. Phys., 81 (1984) 197.
10 M. Labrador, Tesina, University of Barcelona, 1985.
11 M. Labrador, T. Calvet, E. Tauler, M.A. Cuevas-Diarte, E. Estop and Y. Haget, J. Chem. Phys., 84 (1987) 951.
12 T. Calvet, Tesina, University of Barcelona, 1985.
13 T. Calvet, M. Labrador, E. Tauler, E. Estop, M.A. Cuevas-Diarte and Y. Haget, Thermochim. Acta, 147 (1989) 273.